Ocean Systems Engineering, *Vol. 14, No. 4 (2024) 363-381*
https://doi.org/10.12989/ose.2024.14.4.363

Assessing container ship maneuverability in regular waves: A combined experimental and numerical approach

T.V. Rameesha[1a], Kunal N. Tiwari[*1], Akhil Balagopalan[3] and P. Krishnankutty[4]

[1]*KSCSTE National Transportation Planning and Research Center, India*
[2]*National Marine Dredging Company, Abu Dhabi, UAE*
[3]*Admaren Tech Private Limited, India*
[4]*Department of Ship Technology, Cochin University of Science and Technology, India*

(Received August 17, 2024, Revised November 5, 2024, Accepted November 18, 2024)

Abstract. In the traditional assessment of ship maneuvering characteristics, the influence of waves on the hydrodynamic behavior of a ship has been disregarded, despite their capacity to alter the kinematics of the surrounding water particles. This alteration, in turn, affects the hydrodynamic forces acting upon the ship, which ultimately leads to modifications in the vessel's steering and control characteristics. In the present study, a scaled model of a container ship was utilized to conduct free running turning circle maneuvers under varying head sea wave conditions, characterized by different wave heights and lengths. Through these tests, we aim to investigate the effects of wave parameters on the vessel's turning characteristics, thereby advancing our understanding of this critical aspect of naval engineering.

Keywords: KCS; ship maneuvering; turning circle; wave

1. Introduction

Assessing ship maneuverability under wave conditions is crucial in ensuring the safe and efficient operation of ocean-going vessels. While mathematical models have traditionally been used to predict ship maneuvering in calm waters, incorporating the effects of waves in these models is essential to accurately evaluate the performance of a ship in actual sea conditions. The hydrodynamic forces acting on a ship are significantly influenced by waves, resulting in a notable difference in the steering quality of a ship in the presence of waves when compared to calm waters. Therefore, it is imperative that ship designers and naval architects consider wave effects in the evaluation of a vessel's maneuvering characteristics to ensure optimal performance and safety in real-world scenarios.

There exist various methods for investigating the maneuvering properties of a vessel in a seaway, including experimental model testing, unified theory, two-time scale models, and Computational Fluid Dynamics (CFD) techniques. Researchers have utilized these approaches to analyze the impact of waves on ship maneuvering in different ways. For instance, Yasukawa (2006) examined the influence of waves on maneuvering trajectory of a container ship by performing free

∗Corresponding author, Ph.D., E-mail: kunal.n.tiwari@gmail.com

http://www.techno-press.org/?journal=ose&subpage=7 ISSN: 2093-6702 (Print), 2093-677X (Online)

model tests. Xu *et al*. (2007) investigated the effect of varying wave drift forces, such as wave drift added mass and wave drift damping, while conducting Planar Motion Mechanism (PMM) tests in waves. Lee et al. (2009) conducted turning and zig-zag maneuvers on a KVLCC model to study the influence of second-order wave forces on the vessel's maneuvering trajectory. The author found that second-order wave drift forces significantly affect the maneuvering trajectory in waves. Chuang and Steen (2012) carried out free running model tests in regular head sea waves to predict the zig-zag motion, behavior of the azimuth propulsion system, and loss of speed during maneuvering in both calm water and waves.

Theoretical approaches based on the unified theory that encompass both maneuvering and sea keeping aspects were initially proposed by Bailey (1998). Cummins (1962) expressed the unsteady wave memory effects on ship maneuvering in a seaway using a linear convolution integral formulation. Fossen (2005) developed a unified state space model to describe ship maneuvering in a seaway, compactly representing frequency-dependent potential and viscous damping terms using a state space formulation suitable for real-time simulation. Fang *et al*. (2005) developed a simplified six degrees of freedom mathematical model, which combines calm water maneuvering and seakeeping theories, to calculate hydrodynamic forces as a function of encountering frequency in a time-domain simulation. Turning circle tests were simulated for two container ships in different wave height and wave length conditions, and the study highlighted the significant influence of wave height, wave length, and wave direction on the turning trajectory of a ship. Skejic and Faltinsen (2008) studied the maneuvering behavior of a ship in regular waves using a two-time scale model approach. This model combines both seakeeping and maneuvering using slender body theory, where the direct pressure integration method is used to estimate second-order mean drift forces. Zhang *et al.* (2017) developed a numerical simulation method for predicting ship maneuvering in waves based on a two-time scale model method. The predicted turning and zig-zag trajectories for the S175 container ship were compared with free running model test results. The results indicated that incident waves have a significant influence on the maneuvering performance of a ship. The use of numerical methods to investigate maneuvering in waves remains highly challenging due to numerical complexity, and related studies are exceedingly rare. Ferrant (2008) developed SWENCE (Spectral Wave Explicit Navier-Stokes Equations), which incorporates incident flow parameters into the free surface Reynolds Averaged Navier Stokes (RANS) solver ICARE. The present study involves conducting free maneuvering model tests for a container ship (KCS) in regular waves, considering waves with varying heights and lengths. Additional study considered the numerical analysis of another container ship (S175) in waves based on unified state space theory.

2. Free running model experiments in waves

To explain the experimental setup and execution of free running model experiments in waves, it is important to first distinguish between two types of free running models available: wireless controlled models and wire controlled models. The former is a remote controlled model while the latter is positioned under a carriage, with the carriage following the model during free sailing tests. Although wired control models can effectively transfer motor power, control, and measuring signals between the carriage and the model, it is essential to ensure that the arrangement of control cables and other installed equipment does not interfere with the model's free running. For the present case, the wired controlled setup for the free sailing test available at NSTL is utilized.

Table 1 Main particulars of the ship, propeller and rudder

Main particulars	Prototype	Model
Lpp (m)	230.0	3.0464
Lwl (m)	232.5	3.0791
B (m)	32.2	0.4265
D (m)	19.0	0.2517
T (m)	10.8	0.1430
Displacement (m^3)	52030	0.1209
S w/o rudder (m^2)	9530	1.6719
CB	0.651	0.651
CM	0.985	0.98
Propeller		
No. of blades	5	5
D (m)	7.9	0.105
P/D (0.7R)	0.997	0.997
Rudder		
Suraface area (m^2)	115	0.202
Lateral area (m^2)	54.45	0.0096
Turn rate (deg/s)	2.32	20.2

2.1 Experimental setup and test execution

The standard KCS model with a scale ratio of 75.5 is selected for the free running model experiments. The main particulars of the model and prototype are given in Table 1. For free sailing tests, the wave basin should be large enough to allow for free movement. In the present study, free running model tests in calm water are conducted at the Seakeeping and Maneuvering Basin (SMB) facility of Naval Science and Technological Laboratory (NSTL), Visakhapatnam. The wave basin is 135 m long, 37 m wide, and 5 m deep and is fitted with 256 hinged flap type paddles on the longitudinal and transverse direction of the basin. Wave beaches are constructed at the opposite sides of the wave makers. The model is free to move in all six degrees of freedom and is equipped with servo motors for propeller and rudder operations. A dynamometer fitted to the propeller reads the thrust and torque, and a similar one is fitted in the model-rudder arrangement. The longitudinal and vertical center of gravity (LCG and VCG) positions of the bare hull are estimated using a suspension test. The model propeller is run at 990 revolutions per minute (rpm) to achieve a constant speed of 1.4 m/s, which is 98% of the design speed of the model.

Turning circle tests are conducted in both calm water and head sea waves. In the initial phase, the ship moves with a constant speed in a straight course with zero heading angle and rudder angle, which is the approach phase of a turning circle test. Then the rudder angle is deflected to 35° towards port/starboard with a deflection rate of 20.2 degrees/second, which is equal to 2.32 degrees/s in full scale, and is the first phase of the turning circle maneuver. The rudder force and moment produce accelerations that are opposed by the inertial reaction of the ship. Subsequently, hydrodynamic forces are developed, and the ship takes a turn of constant radius as a result of the equilibrium of all force actions on it. This test is repeated in generated regular waves.

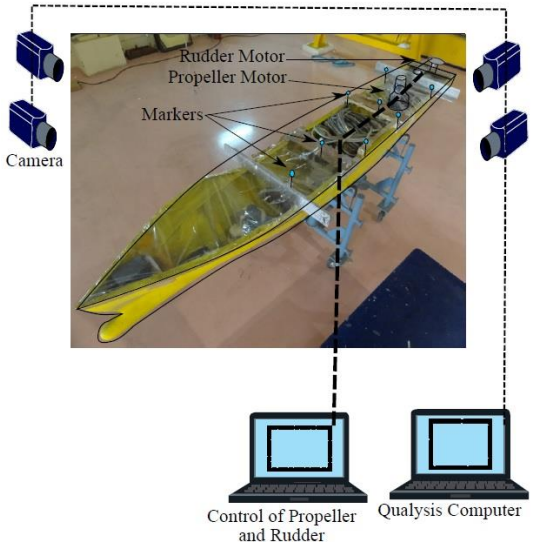

Fig. 1 Arrangement of data acquisition system

To ensure the accuracy of the wave system, the performance of the wave maker is evaluated, and the created waves are calibrated. Wave probes are used to measure the wave heights located along the carriage rails. The position and orientation of the model during model tests are done using a tracking system fitted to the carriage (Fig. 1). The tracking system consists of four Qualysis cameras mounted on the carriage. The cameras can generate infrared pulses, which are reflected from the passive markers mounted on the ship model. A minimum of four markers is required for 3D tracking of the model. For the purpose of our experiment, eight markers were utilized for higher accuracy. The accuracy of the tracking system (1 mm) is comparable to the Differential Global Positioning System (DGPS), which is a commonly used position reference system in full-scale models.

2.2 Experimental results & discussion

The maneuverability and course change capabilities of a vessel can be assessed through the execution of turning circle tests. These examinations are conducted in both still water and in regular head sea waves to identify the impact of different environmental conditions on vessel performance. A depiction of the various stages of the turning circle tests in calm water can be found in Fig. 2.

Tests were performed under a range of wave model conditions, with wave heights of 0.013m, 0.019m, and 0.026m, and wave lengths of 1.5 m, 3 m, 4.5 m, 6.0 m and 7.5 m (corresponding ($\frac{\lambda}{L} = 0.5, 1, 1.5, 2, 2.5.$). Turning parameters were then estimated in head sea wave conditions (hw =0.026 m , λ = 1.5 m) and compared with the outcomes obtained in calm water, as shown in Table 2.

Turning circle trajectory in wave condition is plotted with the trajectory in still water condition for comparison (Fig. 3). Estimated steady turning radius in wave conditions increased by 10.1% compared to still water. Similarly, other parameters such as transfer and tactical diameters also

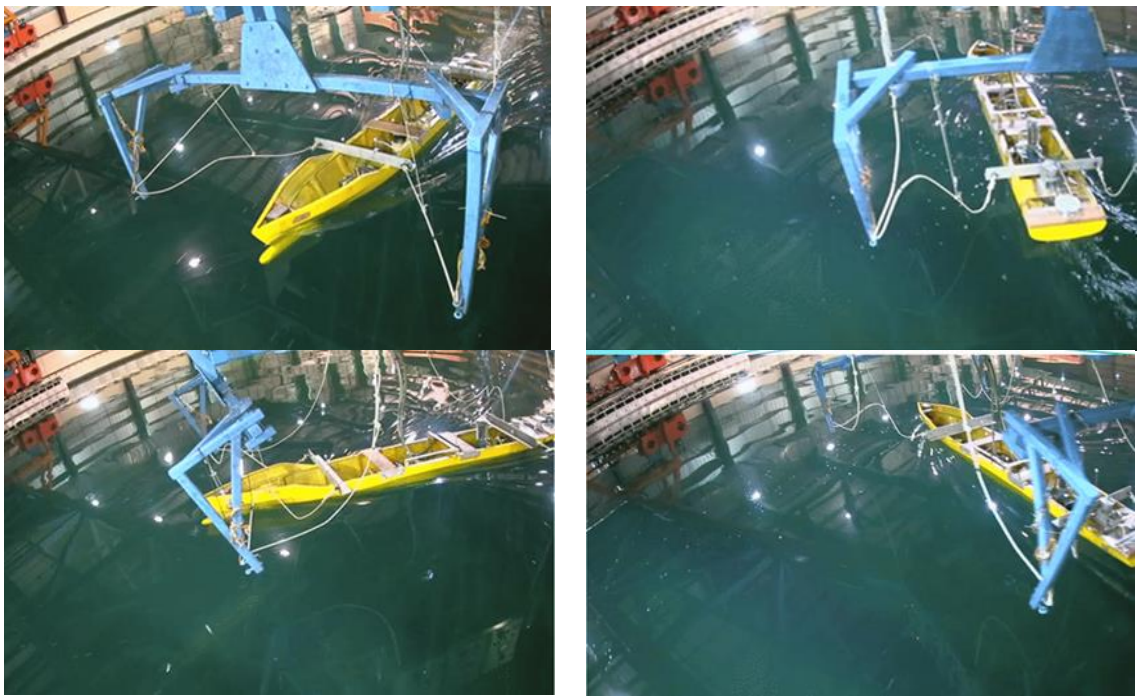

Fig. 2 Model (KCS) position at different stages of turning circle test in calm water

Table 2 Turning parameters in calm water and head wave condition (h_w = 0.026 m, λ =1.5 m)

Turning circle test parameters	Calm water	Wave condition	% deviation wave and calm water condition
Steady turning radius	3.56	3.96	10.1
Transfer	4.65	4.76	2.31
Advance	9.54	7.83	-21.8
Tactical diameter	10.18	10.32	1.35

Table 3 Comparison of turning circle parameters in calm water for KCS container ship

Turning circle parameters	Present study	SIMMAN (2008)
Advance (L_{BP})	3.13 3.34	3.22
Tactical diameter (L_{BP})	3.14	3.48

increased by 2.31% and 1.35%, respectively. However, advance was reduced by 21.8% in head waves compared to the still water condition. This results underscores the significance of wave impact on the turning trajectory of the vessel, suggesting that it should not be neglected.

In the present study, the turning circle trajectory in still water aligned well with results from the SIMMAN 2008 study (Table 3). When comparing the vessel trajectory in calm water to that in waves, it was found that the vessel trajectory tends to drift in the direction of wave propagation.

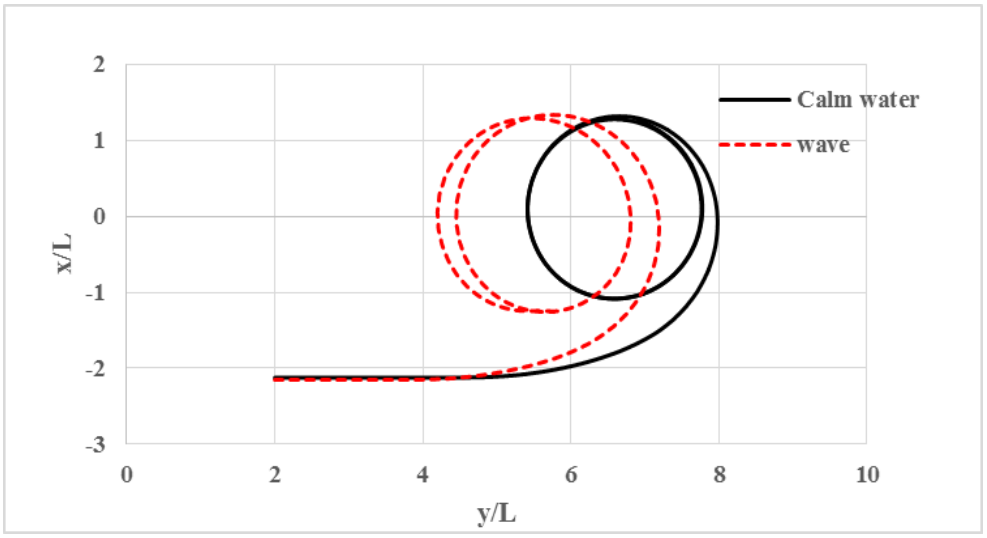

Fig. 3 Turning circle test results in calm water and wave condition for KCS container ship

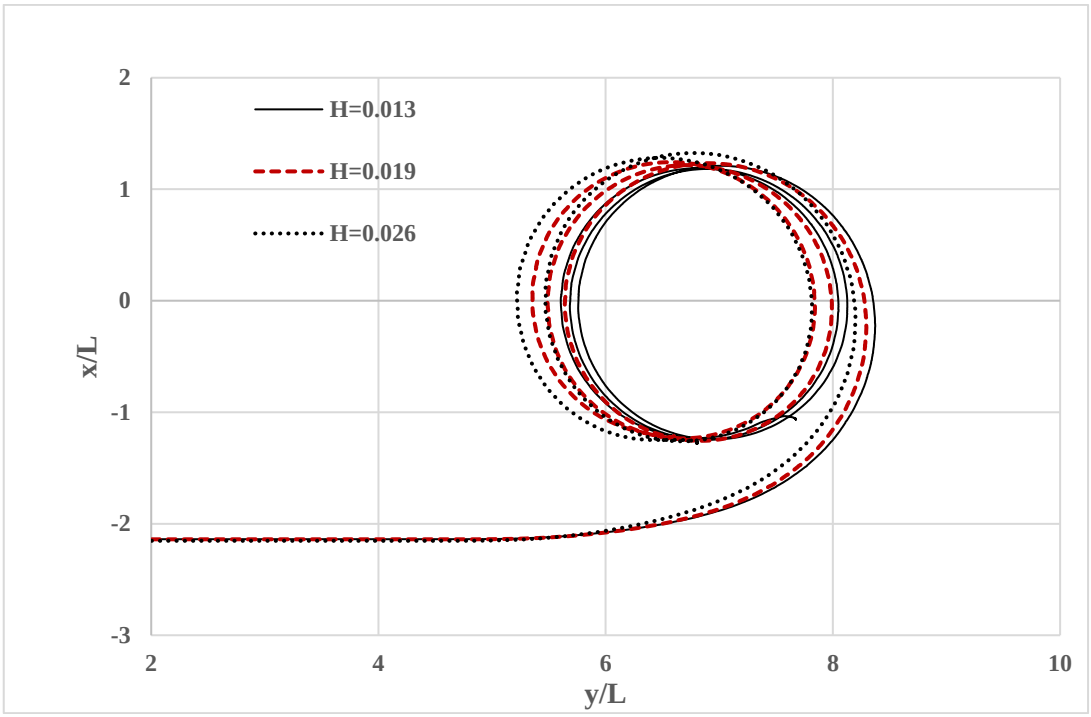

Fig. 4 Turning circle results for different wave lengths for KCS container ship

This drift became more pronounced as the height of the first order wave increased (Table 4 and Fig. 4).

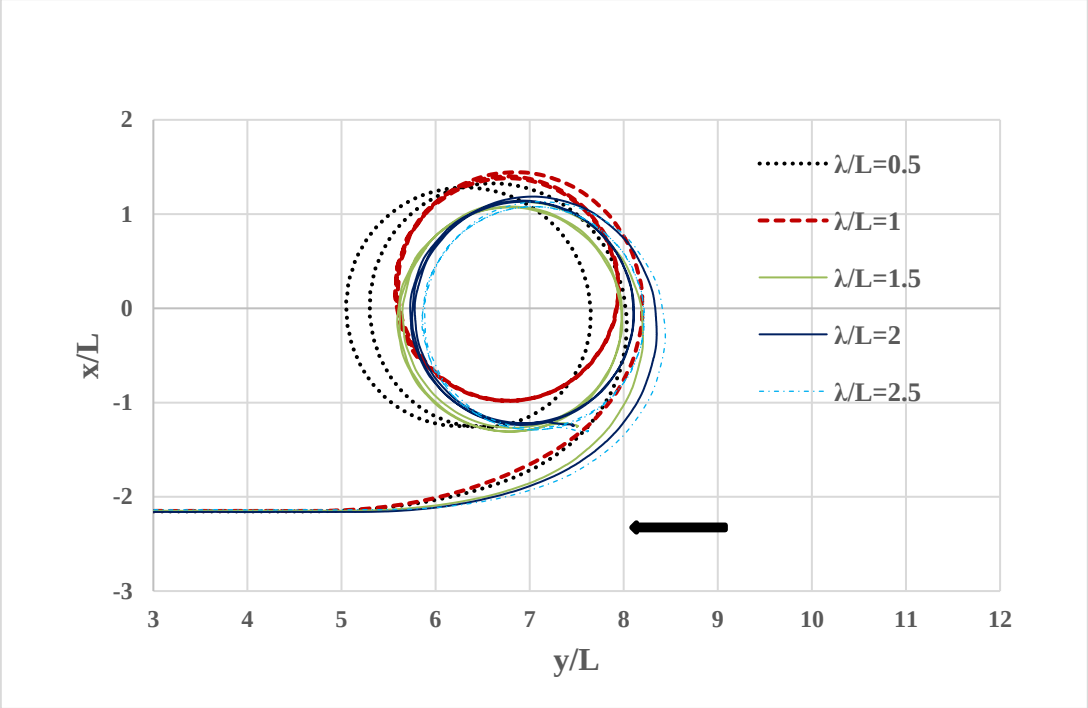

Fig. 5 Turning circle results for different wave lengths for KCS container ship

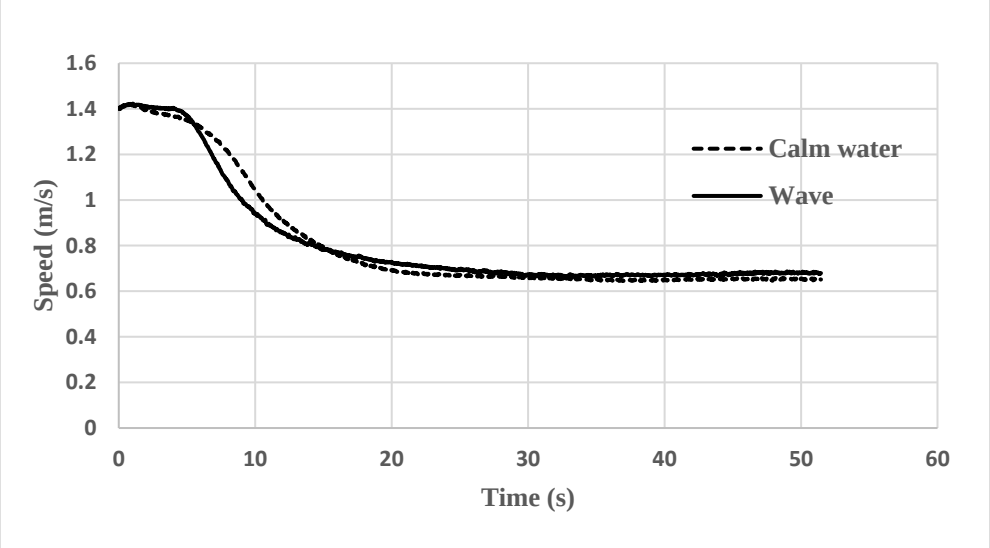

Fig. 6 Speed during turn for turning circle test in calm water and in waves

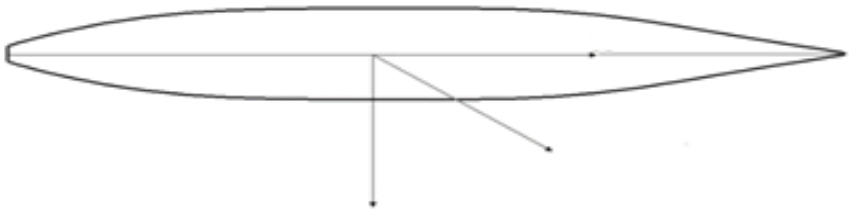

Fig. 7 Maneuvering co-ordinate system (b frame)

Table 4 Turning parameters in different wave heights

Turning circle Test parameters (x/L)	Calm water	Wave height (m)		
		0.013	0.019	0.026
Steady Turning Radius	1.17	1.15	1.26	1.29
Transfer	1.53	1.5	1.51	1.58
Advance	3.13	2.94	2.86	2.79
Tactical Diameter	3.34	3.28	3.31	3.41

Table 5 Turning parameters in different wave lengths for KCS container ship

Turning circle Test parameters (x/L)	Calm water	Wave length λ/L				
		0.5	1	1.5	2	2.5
Steady Turning Radius	1.17	1.23	1.18	1.14	1.018	1.01
Transfer	1.53	1.56	1.72	1.45	1.49	1.46
Advance	3.13	2.57	2.73	2.73	2.88	2.97
Tactical Diameter	3.34	3.39	3.52	3.19	3.18	3.19

The wave length also has a considerable influence on maneuvering trajectory of ship, as detailed in Table 5. Drift of ship towards the wave direction is noticed in wave condition compared to the calm water condition (Fig. 5). Interestingly, longer waves has less effect on turning characteristics of the ship.

The speed during the turning circle test, both in calm water and in waves, has been graphically represented (Fig. 6). These results further underline the influence of sea conditions on vessel maneuverability and emphasize the importance of testing under varied wave conditions.

3. Unified state space model of seakeeping and maneuvering

The ship's maneuvering motion is typically evaluated in still water using a body-fixed reference frame, referred to as the 'b frame' (as illustrated in Fig. 7). In this framework, added mass and

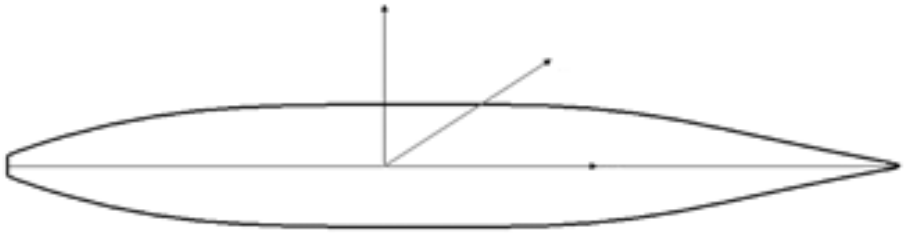

Fig. 8 Wave excitation surge force

damping terms in the equation of motion are estimated under the assumption of zero independent frequency. Conversely, the study of sea keeping encompasses the examination of motion, stability, and control in the presence of wave excitation. The corresponding equations of motion are described from a different perspective, a moving equilibrium frame, known as the hydrodynamic reference frame or the 'h frame' (as shown in Fig. 8).

The body-fixed frame, or the 'b frame', positions its coordinate origin at the center of gravity, denoted as 'G'. The x-axis in this frame extends positively towards the bow, the y-axis is positive towards the starboard, and the z-axis is directed downwards. Hydrodynamic forces and moments are calculated with respect to the moving hydrodynamic reference frame, which follows the path of the ship.

In contrast, the coordinate origin of the 'h frame', or hydrodynamic reference frame, is located at the mean water line, marked as 'o'. Within this frame, the x-y plane runs parallel to the still water surface, and the ship performs oscillations around this moving frame. The x-axis extends positively forward, the y-axis is positive towards the portside, and the z-axis is directed upwards.

A unified state space model was proposed by Fossen in 2005, which seamlessly integrates both sea keeping and maneuvering theories. This model utilizes impulse response functions and convolution integrals to express the fluid memory effect in the equations of motion. This comprehensive model provides a holistic view of the vessel's behavior, taking into account both the inherent maneuvering properties of the ship and the influences of external wave excitations.

3.1 Mathematical model

In this study, we apply the nonlinear steering model put forward by Son and Nomoto in 1981. As our test subject, we employ a container ship, specifically an S175 model. The key characteristics of this ship model are outlined in Table 6.

The original mathematical model employed in still water conditions has been adapted for wave conditions. This modification involved considering a linear coupled derivative within the three degrees of freedom equation of motion. The modified equation of motion are given in Eqs. (1) to (3). By incorporating wave conditions into our mathematical model, we aim to capture a more realistic representation of the vessel's behaviour, taking into account the complex dynamics brought on by wave interactions. This comprehensive approach provides a valuable insight into the vessel's performance under varied environmental conditions, furthering our understanding of marine maneuverability.

Equations of motion in waves that involving frequency-dependent derivatives often fall short in

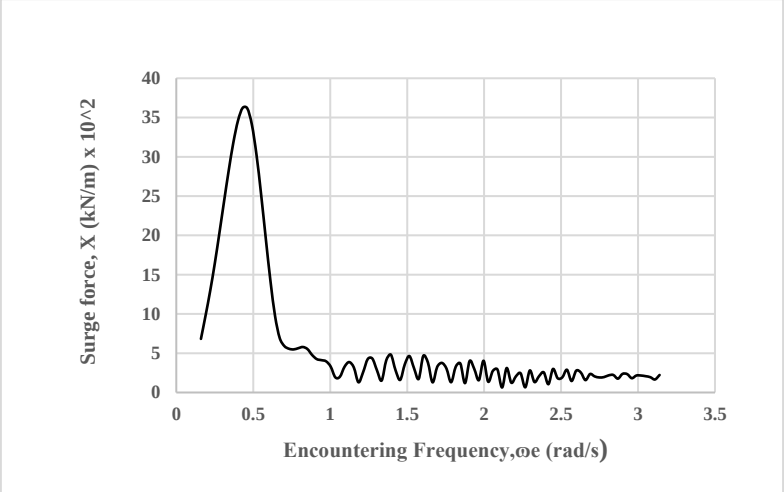

Fig. 9 Wave excitation surge force

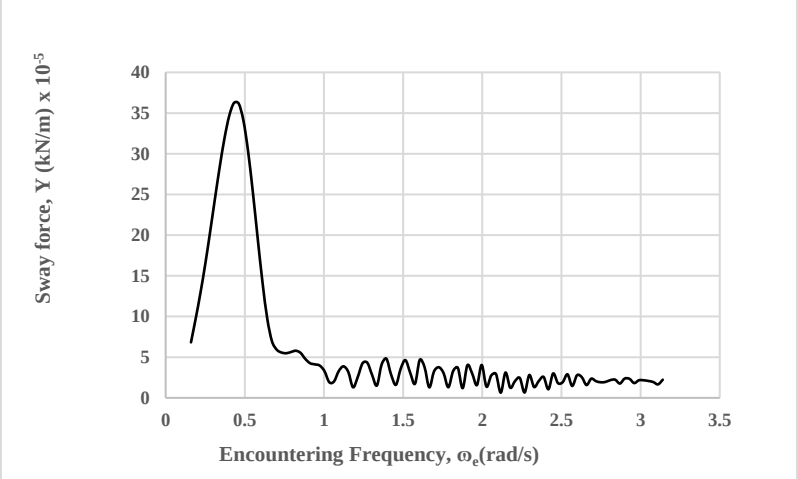

Fig. 10 Wave excitation sway force

accurately representing the forced response of a ship. Consequently, these frequency-dependent derivatives can be transformed into a more fitting time domain representation using impulse response functions, as proposed by Cummins in 1962. Memory effect of fluid can be captured using convolution integral which describes how fluid motion at a given time depends on the past history of motion. The retardation function, which determines the fluid response to an impulsive sway velocity of the ship, denoted as v(τ), can be calculated using the Response Amplitude Operator (RAO). This function essentially describes how the fluid's past behavior influences its present state, thereby factoring in the fluid's 'memory' of past states into its current response.

$$[m - X_{\dot{u}}(\infty)]\dot{u} = (1 - t_R)T_p + X_\delta sin\delta + f_x \sin(\omega_e t + \varepsilon) \quad (1)$$

$$\left(m - Y_{\dot{v}}(\infty)\right)\dot{v} - Y_{\dot{r}}\dot{r} - Y_v(\infty)v - Y_r(\infty)r + \int_0^t Y_v(t-\tau)\,v(\tau)d\tau + \int_0^t Y_r(t-\tau)\,r(\tau)d\tau = Y_\delta \cos\delta + f_Y \sin(\omega_e\, t + \varepsilon) \quad (2)$$

$$(I_Z - N_{\dot{r}})\dot{r} - N_{\dot{v}}(\infty)\dot{v} - N_v(\infty)v - N_r(\infty)r + \int_0^t N_v(t-\tau)\,v(\tau)d\tau + \int_0^t N_r(t-\tau)\,r(\tau)d\tau = N_\delta \cos\delta + m_z \sin(\omega_e\, t + \varepsilon) \quad (3)$$

Furthermore, the retardation function can be derived in terms of acceleration or damping derivatives, offering additional methods for quantifying this fluid response. This comprehensive approach ensures a nuanced and precise depiction of ship behavior, accommodating the complex dynamics introduced by fluid memory effects. The retardation functions are given in Eqs. (4) to (7).

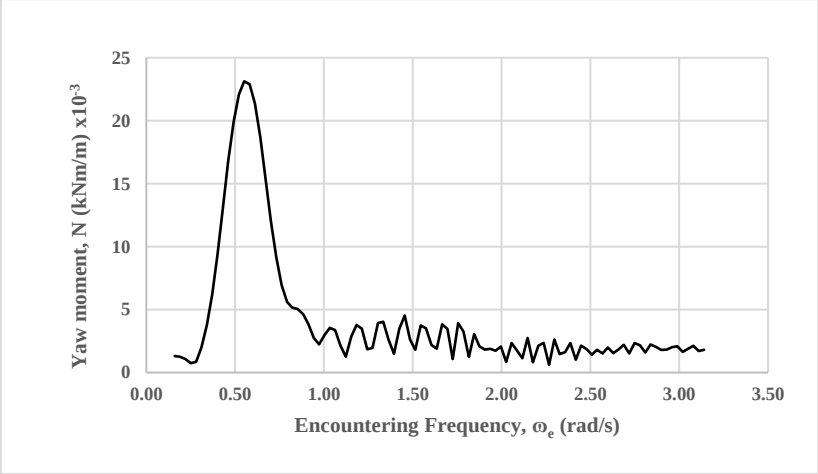

Fig. 11 Wave excitation yaw moment

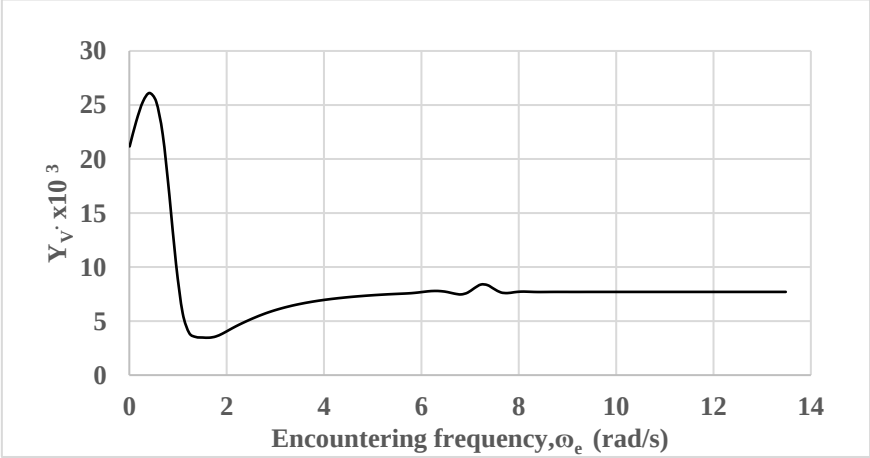

Fig. 12 Variation of $Y_{\dot{v}}$ with encountering frequency ω_e

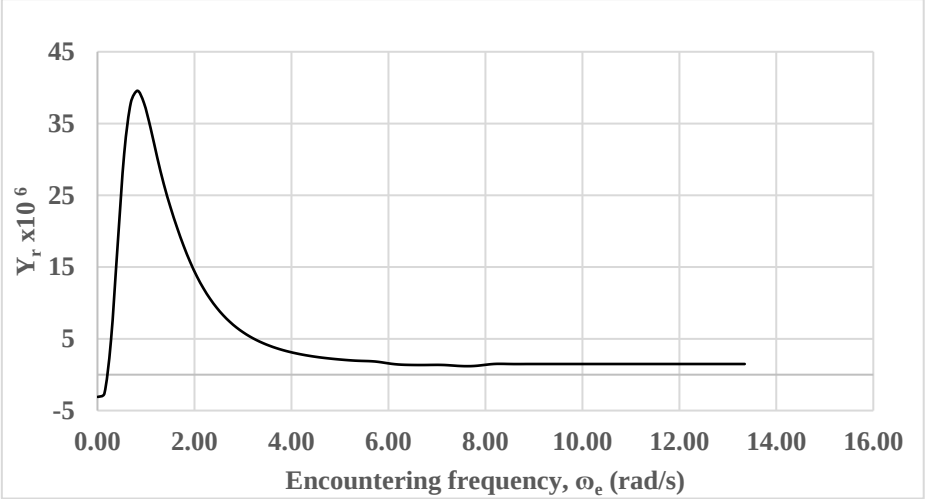

Fig. 13 Variation of Y_r with encountering frequency

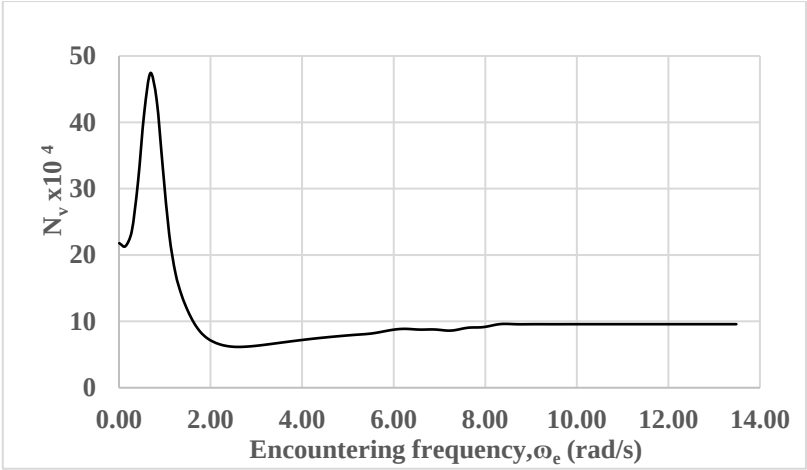

Fig. 14 Variation of N_v with encountering frequency ω_e

$$Y_v(t) = \frac{2}{\pi}\int_0^\infty [Y_v(\omega) - Y_v(\infty)]cos\omega t d\omega \tag{4}$$

$$Y_{\dot{v}}(t) = \frac{2}{\pi}\int_0^\infty \omega[Y_{\dot{v}}(\omega) - Y_{\dot{v}}(\infty)]sin\omega t d\omega \tag{5}$$

$$Y_{\dot{v}}(\infty) = \frac{2}{\pi}\lim_{\omega\to\infty} Y_{\dot{v}}(\omega) \tag{6}$$

$$Y_v(\infty) = \lim_{\omega\to\infty} Y_v(\omega) \tag{7}$$

In the mathematical model used, u and v represent linear velocities in the x and y directions, respectively. The angular velocity in the z direction is symbolized by 'r'. $\dot{u}$ and $\dot{v}$ indicate linear

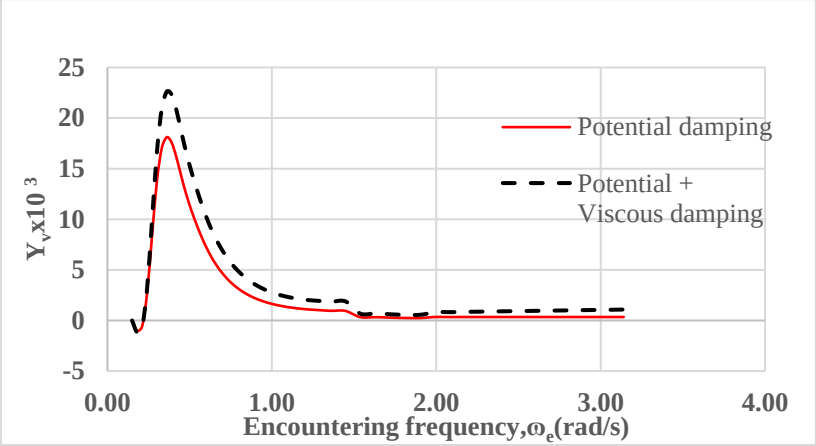

Fig. 15 Variation of Y_v with encountering frequency

acceleration in the x and y directions, respectively, while $\dot{r}$ denotes the angular acceleration in the z direction.

The mass of the ship is represented by 'm', while I_z refers to the mass moment of inertia of the ship about the z-axis. The thrust deduction factor is designated by t_p, the propeller thrust is T_p, and the rudder angle is represented by δ.

The derivatives of forces or moments due to rudder deflection are symbolized as X_δ, $Y_\delta$and N_δ. The contributions of wave excitation forces and moments in the x, y, and z directions are represented f_x , f_y and m_z, respectively. Lastly, ω denotes the wave frequency, while ω_e represents the encountering frequency.

The model provides a clear, comprehensive framework for analysing and understanding the complex dynamics of ship maneuvering and response in wave conditions.

3.2 Wave excitation forces and maneuvering derivatives

Wave excitation forces acting on the container ship when moving at a constant speed in head sea conditions are estimated using SEAWAY, a 2D-strip theory-based program developed by Journée and Adegeest (2003). The relevant data are presented in Figs. 9 to 11.

In the equations of motion, added mass and damping coefficients for a ship in wave conditions are frequency-dependent. These derivatives are estimated using the 2D-strip theory-based program within a hydrodynamic reference frame, while the maneuvering motions are simulated with respect to a body-fixed frame.

The transformation from the hydrodynamic frame ('h frame') to the body-fixed frame ('b frame') typically depends on rotational oscillations in the x, y, and z directions. Considering the three degrees of freedom motion in surface ship maneuvering, yaw oscillation is taken into account and the rotation matrix in yaw is near the identity matrix (Fossen 2005).

Strip theory is predicated on potential theory, which is formulated under the assumption of a fluid continuum considered as inviscid. Potential coefficients are often calculated using a seakeeping program; however, they do not provide an accurate representation of the frequency response unless viscous damping is included (Fossen 2005).

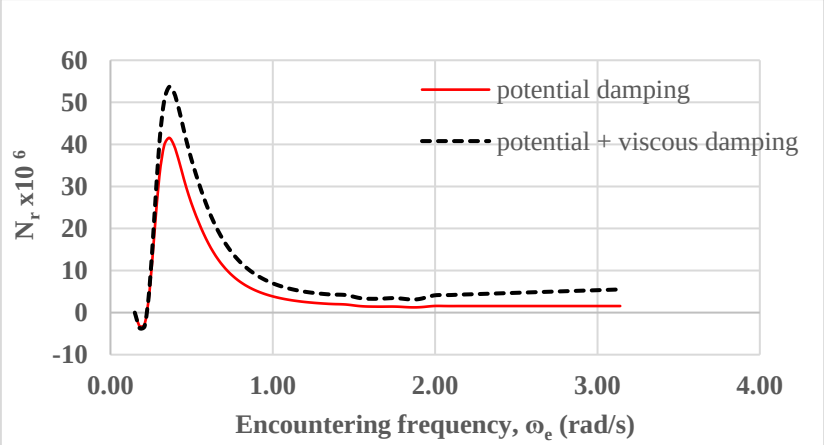

Fig. 16 Variation of N_r with encountering frequency ω_e

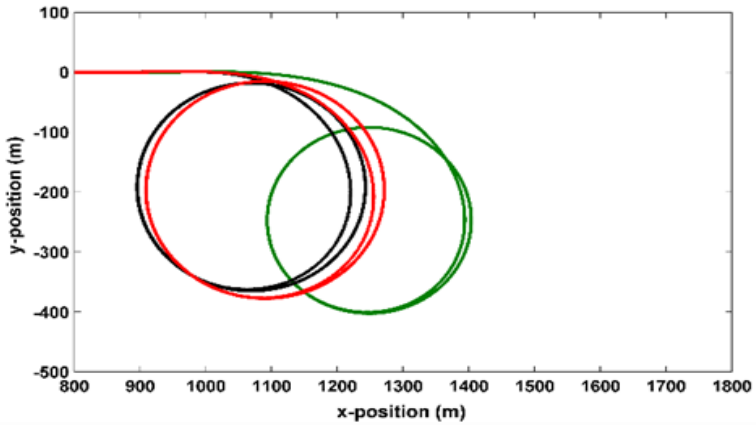

Fig. 17 Turning circle test results in regular waves for S175 containership

Hence, to account for the effects of viscous damping, we employ a viscous ramp function proposed by Bailey in 1997 (Eq. (8)). This function allows for an approximate determination of the viscous effects of the diagonal damping derivatives, namely Y_v and N_r.

$$Y_v^{visc}(\omega) = Y_v \left(1 - \frac{\omega}{\omega_v}\right), \quad \omega \leq \omega_{v,}\ i = 1 \ldots .6 \tag{8}$$

ω is the wave frequency at which Y_v is calculated, Y_v^{visc} is the viscous effected hydrodynamic derivative. ω_v is the minimum wave frequency at which Y_v become zero.

Hence

$$Y_v^{visc}(0) = Y_v \tag{9}$$

$$Y_v^{visc}(\omega_v) = 0 \tag{10}$$

Wave

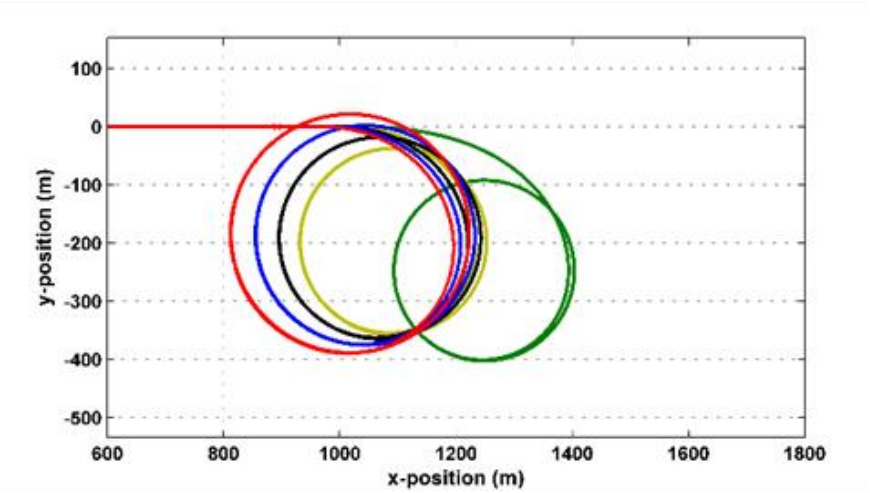

Fig. 18 Turning circle test results in regular waves for S175 container ship

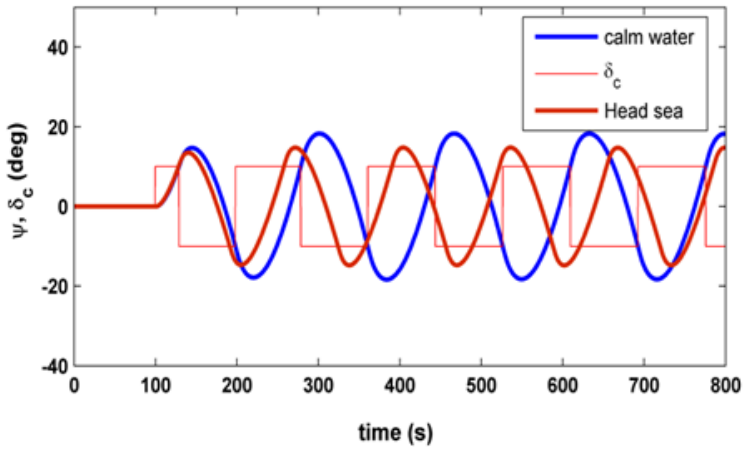

Fig. 19 $20^0/20^0$zig-zag maneuver in head sea condition for S175 container ship

N_r can also be calculated using the same equations.

3.2 Results and discussion

The added mass and damping derivatives are graphically represented against the encountering frequency in Figs. 12 to 14. Including viscous effects, the diagonal damping derivatives, Y_v and

Table 7 Turning circle parameters in different wave height

Turning circle Test parameters (m)	Calm water	Wave height, H (m)				% change between wave (H_w=2 m) and calm water conditions.
		1	1.5	2	2.5	
Steady Turning Radius	155	145	150	156	164	0.6
Transfer	132	87	90	94	99	-40
Advance	444	331	332	335	338	-32
Tactical Diameter	363	320	331	345	363	-5

N_r, are plotted against the encountering frequency in Figs. 15 and 16.

The frequency-dependent hydrodynamic derivatives in the modified equations of motion for the wave condition (Eqs. (1)-(3)) are calculated using the strip theory program. It was observed that these derivatives stabilize and become constant after a particular encountering frequency is reached.

For the purpose of maneuvering simulation, this steady value of hydrodynamic derivatives is incorporated into the equations of motion.

In order to represent these derivatives in the time domain, which is a requisite for the maneuvering simulation, Eqs. (1)-(3) are transformed into integral equations using convolutions. Wave excitation forces are estimated and subsequently included in the equation of motion at each time step of the maneuvering simulation.

In the context of still water conditions, rudder and propeller forces are approximated using empirical relations. For this particular study, we do not consider the effects of waves on these forces. This simplification allows us to focus our analysis on the central factors affecting the ship's maneuvering characteristics.

Standard maneuvering tests, such as turning and zigzag tests, are generally numerically simulated to study a vessel's maneuvering capabilities. These tests provide insights into the vessel's turning and course-changing characteristics. In this study, we have simulated turning and zigzag maneuvers for a vessel in head wave conditions.

We compared the turning trajectory parameters for the S175 container ship with those observed in calm water conditions, as reported by Son and Nomoto (1981) for the same ship (refer to Fig. 20). The trajectory was simulated using both potential and viscous damping derivatives. We found that the turning trajectory in waves tends to drift towards the wave direction, as compared to calm water.

Turning circle simulations were conducted for various wave heights, such as H_w=1 m, 1.5 m, 2 m, and 2.5 m. The effects of wave height on turning circle parameters are compared in Fig. 21 and Table 7. As the wave height increased, we observed a noticeable drift of the ship towards the direction of the incident wave during the turning circle maneuver.

The present results align with the trend demonstrated by Fang *et al*. (2005), who studied the effect of head sea conditions on two container ships. The findings also matches with the model proposed by Hamamoto *et al.* (1994), which considered only linear derivatives for maneuvering prediction.

Zigzag maneuvers with a configuration of 20°/20° were simulated for both calm water and

head sea wave conditions, with a wave height of 1.5 m (Fig. 19). We found that the computed zigzag trajectory in head waves tends to drift towards the direction of the incident wave, in comparison to calm water conditions.

4. Conclusions

This study combined experimental and numerical investigations to analyze the impact of wave conditions on maneuvering trajectory two different container ships. Employing the Seakeeping and Maneuvering Basin (SMB) facility at the Naval Science and Technological Laboratory (NSTL) in Visakhapatnam, free-running model tests were performed. The mathematical model proposed by Son and Nomoto (1981) was modified for wave conditions, with a linear coupled derivative incorporated in the three degrees of freedom. From the present study, the

- Results indicated a vessel drift towards the direction of wave propagation under wave conditions, with an intensification of drift observed with increased wave steepness (H/λ).
- A decrease in drift was noted with increased wave length (λ/L from 0.5 to 0.25).
- The research focus was limited to head waves, underlining the need for more extensive studies considering waves from varied directions.
- There is a notable gap in current International Maritime Organization (IMO) regulations, which are primarily catered to calm water conditions. Given the prevailing wave conditions under which ships operate, it is crucial to revise these guidelines.
- A clear understanding of ship controllability in seaway conditions is essential for operational safety, calling for the inclusion of wave effects in IMO regulations.

Acknowledgments

The authors would like to express their gratitude to NSTL in allowing to use the Seakeeping Maneuvering Basin (SMB) to conduct free running model tests and also to Naval Research Board (NRB), India in sponsoring the above project.

References

Bailey, P.A. (1997), "A unified mathematical model describing the maneuvering of a ship travelling in a seaway", *Trans. RINA*, **140**, 131-149.

Chuang, Z. and Steen, S. (2012), "Speed loss due to seakeeping and maneuvering in zigzag motion", *Ocean Eng*., **48**, 38-46. https://doi.org/10.1016/j.oceaneng.2012.04.009.

Cummins, W.E. (1962), The impulse response function and ship motions (No. DTMB-1661). David Taylor Model Basin Washington DC.

Fang, M.C., Luo, J.H. and Lee, M.L. (2005), "A nonlinear mathematical model for ship turning circle simulation in waves", *J. Ship Res*., **49**(2), 69-79. https://doi.org/10.5957/jsr.2005.49.2.69.

Ferrant, P., Gentaz, L., Monroy, C., Luquet, R., Ducrozet, G., Alessandrini, B. and Drouet, A. (2008), "Recent advances towards the viscous flow simulation of ships manoeuvring in waves", *Proceedings of the 23rd International Workshop on Water Waves and Floating Bodies*, Jeju, Korea.

Fossen, T.I. (2005), "A nonlinear unified state-space model for ship maneuvering and control in a seaway", *Int. J. Bifurcation Chaos*, **15**(9), 2717-2746. https://doi.org/10.1142/S021812740501369.

Hamamoto, M., Matsuda, A. and Ise, Y. (1994), "Ship motion and the dangerous zone of a ship in severe following seas", *J. Soc. Naval Archit. Japan*, (175), 69-78. https://doi.org/10.2534/jjasnaoe1968.1994.69.

Journée, J.M.J. and Adegeest, L.J.M. (2003), Theoretical manual of strip theory program "SEAWAY for Windows". TU Delft Report 1370.

Lee, S.K., Hwang, S.H., Yun, S.W., Rhee, K.P. and Seong, W.J. (2009), "An experimental study of a ship manoeuvrability in regular waves", *Proceedings of the International Conference on Marine Simulation and Ship Maneuverability*, Panama.

Skejic, R. and Faltinsen, O.M. (2008), "A unified seakeeping and maneuvering analysis of ships in regular waves", *J. Mar. Sci. Tech*., **13**(4), 371-394. https://doi.org/10.1007/s00773-008-0025-2.

Son, K.H. and Nomoto, K. (1981), "On the coupled motion of steering and rolling of a high speed container ship", *J. Soc. Naval Archit. Japan*, **150**, 73-83. https://doi.org/10.2534/jjasnaoe1968.1981.150_232.

Stern, F., Agdrup, K., Kim, S.Y., Hochbaum, A.C., Rhee, K.P., Quadvleig, F., Perdon, P., Hino, T., Broglia, R. and Gorski, J. (2011), "Experience from SIMMIAN2008-The first workshop on verification and validation of ship maneuvering simulation methods", *J. Ship Res*., **55**(2), 135-147. https://doi.org/10.5957/jsr.2011.55.2.135.

Xu, Y., Bao, W., Kinoshita, T. and Itakura, H. (2007), "A PMM experimental research on ship maneuverability in waves", *Proceedings of the 26th International Conference on Offshore Mechanics and Arctic Engineering*, American Society of Mechanical Engineers.

Yasukawa, H. (2006), "Simulations of ship maneuvering in waves (1 st report: turning motion)", *J. Japan Soc. Naval Archit Ocean Engineers*, **4**, 127-13.

Zhang, W., Zou, Z.J. and Deng, D.H. (2017), "A study on prediction of ship maneuvering in regular waves", *Ocean Eng*., **137**, 367-381. https://doi.org/10.1016/j.oceaneng.2017.03.046.

RS

Nomenclature

A	Horizontal distance between two strings(m)
B	Beam (m)
D	Depth (m)
f_x	Surge force amplitude (kN/m)
f_y	Sway force Amplitude (kN/m)
h_w	Wave height (m)
I_{xx}	Moment of inertia in X direction
I_{ZZ}	Moment of inertia in Z direction
k_{zz}	Radius of gyration in z-direction (m)
L_{BP}	Length between perpendiculars(m)
l	length of cable from its point of support to the point of its attachment to the model
m	Mass of the ship (kg)
m_z	Yaw moment amplitude
N_δ	Rudder derivative in z- direction
$N_{\dot{r}}$	Hydrodynamic coupled derivative with respect to yaw acceleration
N_r	Hydrodynamic linear coupled derivative of yaw moment with respect to yaw rate
$N_{\dot{v}}$	Hydrodynamic coupled derivative of yaw moment with respect to sway acceleration
N_v	Hydrodynamic linear coupled derivative of yaw moment with respect to sway velocity
r	Yaw rate (rad/s)
$\dot{r}$	Yaw acceleration (rad/s^2)
t_R	Thrust deduction factor
T	Average period of oscillation in Bifilar suspension test
T_p	Propeller Thrust
T_a	Draft at the aft end (m)
T_m	Mean draft (m)
T_f	Draft at the fore end (m)
u	Linear velocity in surge direction (m/s)
$\dot{u}$	Linear acceleration in surge direction(m/s^2)
v	Linear velocity in sway direction (m/s)
$\dot{v}$	Linear acceleration in sway direction(m/s^2)
X_δ	Rudder deflection derivative in x-direction
$X_{\dot{u}}$	Hydrodynamic coupled derivative in surge with respect to surge acceleration.
Y_δ	Rudder deflection derivative in y- direction
$Y_{\dot{v}}$	Hydrodynamic coupled derivative of sway force with respect to sway acceleration
Y_v	Hydrodynamic linear coupled derivative of sway force with respect to sway velocity
Y_r	Hydrodynamic linear coupled derivative of sway force with respect to yaw rate
∇	Displaced volume (m^3)
ω	Wave frequency (rad/s)
ω_e	Encountering frequency(rad/s)
ω_v	Wave frequency at which hydrodynamic derivative become zero (rad/s)
ε	Phase angle (rad) between ship motion and wave motion
δ	Rudder angle(rad)
λ	Wave length (m)